Optica Applicata, Vol. XLII, No. 1, 2012
DOI: 10.5277/oa120111

Research and fabrication of integrated optical chip of Mach–Zehnder microinterference accelerometer

TANG DONG-LIN*, DAI BING, HE SHAN, XIAO KUN-QING, ZHANG LIANG, WANG PENG

Key Laboratory for Petroleum-gas Equipment of EMC, Southwest Petroleum University, Chengdu 610500, China

*Corresponding author: xnsytdl@yahoo.com.cn

A novel hybrid-integrated optical accelerometer, based on Mach–Zehnder interference, is described. The integrated Mach–Zehnder microinterferometer chip is investigated theoretically and experimentally. On the $LiNbO_3$ substrate with the dimensions of 38 mm×6 mm×2 mm, MMI optical power splitter, Y-branching guide, phase modulator and polarizers are integrated to constitute the Mach–Zehnder microinterference chip. The performance of a prototype of the accelerometer is characterised. The measured frequency spectrum is in good agreement with the theoretical prediction.

Keywords: integrated optics, Mach–Zehnder microinterference chip, accelerometer, Ti:$LiNbO_3$ waveguide.

1. Introduction

Integrated (hybrid-integrated) optical accelerometers (IOA) are interest growing interest in a variety of application fields. Their reduced dimensions and weight together with the possibility of low-cost mass production make them ideal in a wide field range: automation technology, earth and sky observation, till safety and security [1–3]. In the previous papers, several fiber-optic accelerometers have been demonstrated, in which single-mode all-fiber Mach–Zehnder [4], Fabry–Pérot [5], and Michelson interferometers [6] were employed to detect the phase changes induced by the externally applied acceleration. Those sensing systems tend to occupy a relatively large area and to require precise alignment of the optical components. A solution to these problems is the integration of the optical components for the sensing onto a substrate. This integrated optic sensor has several advantages such as compactness, lightness, alignment-free configuration and potentially efficient interaction between the lightwave and the measurand. There have been several proposals of integrated optical accelerometers. For example, GORECKI had realized a silicon-based microinterferometer with significant SAW phase modulation, performed by deposition of a ZnO

thin film transducer [7], LLOBERA *et al.* designed an optical accelerometer based on antiresonant waveguides, which has an optical sensitivity of 4.6 dB/g [8].

In this paper, based on our previous work on Mach–Zehnder fiber-optical accelerometer for seismic prospecting [9], we present a novel high-performance hybrid-integrated fiber-optic accelerometer employing an integrated optical Mach––Zehnder interferometer using single-mode Ti:$LiNbO_3$ waveguides. Three polarizers and two phase modulators are integrated with the Mach–Zehnder interferometer fabricated by integrated optics technology on the same $LiNbO_3$ substrate. The accelerometer with the resonant frequency of 3416 Hz and sensitivity of 3.22×10^{-3} rad/m/s^2 ($a = 0.2g$ (1.96 m/s^2)) is demonstrated to work well in the range of 100–3000 Hz. It can be employed to monitor or accurately measure vibrations in various areas such as seismic measurements in geophysical survey, *etc*.

2. Principle of accelerometer operation

Figure 1 shows a hybrid-integrated fiber-optic accelerometer, which consists of four parts: the input elements (laser, fiber and V-grooves), the Mach–Zehnder microinterferometer (MZI) chip (polarizer, MMI optical power splitter, mass, Y-branch waveguide, phase modulator, polarizers), the output elements (fiber, V-grooves and two PIN photodiodes) and the signal processing system.

A light beam of intensity I, coupled from the fiber to the V-grooves, is split by the MMI optical power splitter into four beams of equal intensities which propagate in the arms of the MZI chip. After traversing the arms of the MZI chip, the beams merge at the output Y-junction and produce interference fringes based on the applied acceleration which is observed at the output port. Two PIN photodiodes are employed to convert interferometric optical intensity into electric signal, which is subsequently proceeded by the signal processing system.

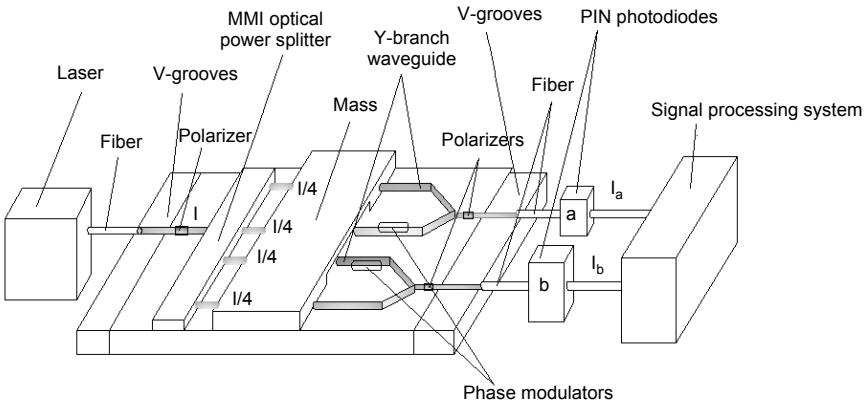

Fig. 1. Sketch of the hybrid-integrated fiber-optic accelerometer.

3. Mach–Zehnder microinterferometer (MZI) chip

A schematic of the Mach–Zehnder microinterferometer (MZI) chip, the key element of the accelerometer, is shown in Fig. 2.

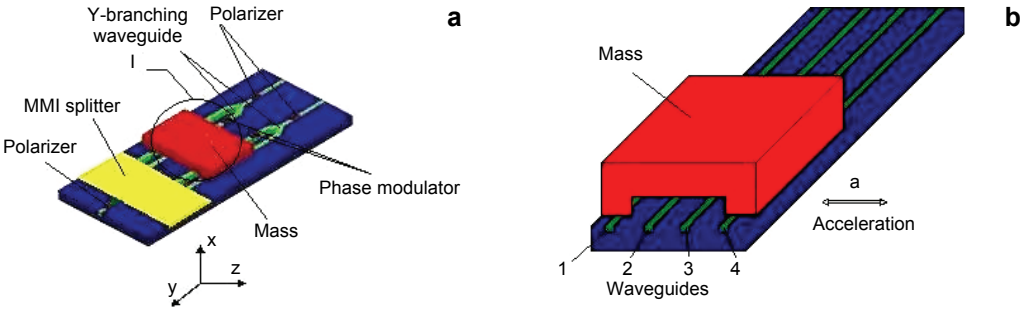

Fig. 2. Schematic of the Mach–Zehnder microinterferometer (MZI) chip. Top view of the chip (**a**) and enlarged view of region I (**b**).

A light beam, which is polarized perpendicular to the stress direction caused by the acceleration forces on proof mass, is split by MMI splitter forming four separate beams traveling in waveguides 1, 2, 3, and 4, each with the intensity of $I/4$. When the proof mass attached to waveguides 1 and 4 is accelerated with acceleration forces in the direction of ΔF, it will stress one waveguide in tension and the other in compression. This changes the index of refraction of these photoelastic waveguides. The phase shift following the variation of the index will be adjusted by external acceleration. The light passing through waveguides 2 and 3, which are not stressed, passes through 90° phase modulators. The light which is modulated by external acceleration and the phase modulator will pass through polarizers after being coupled by the Y-branching waveguide. The polarizers are employed to realize and maintain the polarization state of the output lightwaves, and also to filter the optical signals out of detection directions. The light signals are converted to electrical signals by photodetectors. Acceleration is achieved by feeding the electrical signal into a signal processor unit.

Having obtained the change of refractive index of the waveguide, we can obtain the phase shift caused by the applied acceleration:

$$\Delta\phi = \frac{2\pi}{\lambda}\Delta n\, l = \frac{2\pi B m \Delta a}{w\lambda} \tag{1}$$

where, $\Delta\phi$ is the phase shift, Δn is the change of refractive index, m is the proof mass, Δa is the change in acceleration, B is the photoelastic constant of $LiNbO_3$, $B = 5.78\times10^{-12}$ m^2/N, w is the width of waveguide.

Since there is a 90° phase lag between beams, the equation for beam intensity at the PIN photodiode is:

$$I_{\text{out}} = \frac{I}{2}\left[1 + \cos(\Delta\phi - 90°)\right] = \frac{I}{2}\left[1 + \sin(\Delta\phi)\right] \tag{2}$$

where I is the input laser intensity. The signal input to signal processor from PIN photodiode (a) may be

$$I_a = \frac{I}{2}\left[1 + \sin(\Delta\phi)\right] \tag{3}$$

and the signal input from PIN photodiode (b) may be

$$I_b = \frac{I}{2}\left[1 - \sin(\Delta\phi)\right] \tag{4}$$

with the acceleration ΔF in one direction. For acceleration forces in the opposite direction only the signs (+ or –) will change.

If the two signals are normalized, the difference of output signal from the signal processor is:

$$\frac{I_a - I_b}{I_a + I_b} = \sin(\Delta\phi) \tag{5}$$

which is proportional to the input acceleration.

The sensitivity S is:

$$S = \frac{\Delta\phi}{\Delta a} = \frac{2\pi B m}{w\lambda} \tag{6}$$

In our design, a typical example may be: light axis $n_0 = 2.219$, $n_e = 2.145$. When the wavelength of polarized light (λ) is 1.3 μm, the waveguide geometry sizes of the sensors are: L = 10 mm, w = 6.5 μm, h = 2.5 μm, the proof mass m = 100 g, and the sensitivity of the sensor is 3.22×10^{-7} rad/m/s^2.

4. Fabrication and experimental results

The high-quality Mach–Zehnder microinterferometer chip was prepared on $LiNbO_3$ substrates with the use of Ti in-diffusion techniques [10].

In order to minimize the loss, an MMI coupler is selected as the power splitter. The MMI width (W) is chosen as 116.33 μm to ensure easy separation between the four output ports. The first mirrored-image position of TE polarizations can be found at 68.52 μm according to the BPM results. After properly choosing the param-

eters of the MMI coupler, the simulation shows that the propagation loss decreases to only 0.3 dB.

It is important in the interferometry to keep the polarization state of the two interfering beams the same [11], so three Al-shielded polarizers with the length of 5 mm, prior to the SiO_2 buffer layer with the thickness of 50 nm, are designed on the microinterferometer to realize and maintain TE mode polarized lights.

Considering the hybrid-integrated optical accelerometer response and fabricating craft, we adopt the lumped waveguide phase modulator [12] shown in Fig. 3, which is integrated on the *X*-cut and *Y*-propagation $Ti:LiNbO_3$ substrate, in which TE mode is transmitted and the maximal electro-optic coefficient γ_{33} is obtained.

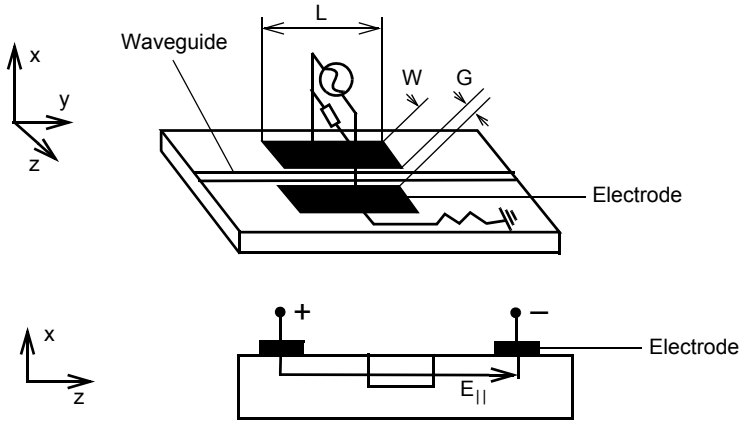

Fig. 3. Lumped waveguide phase modulator.

According to theoretical analysis and the-state-of-the-art, the structure has been designed as follows: electrode voltage $V = 2.5000$ V, electrode length $l = 7.9910$ mm, guides width $w = 5.8312$ μm, electrode interval $G = 18.5000$ μm, electrode thickness $t = 0.4000$ μm, electrode capacitance per unit length $C_0 = 2.0769$ pF/cm, electrode capacitance 1.6596 pF, electrode bandwidth $\Delta f = 3.8359$ GHz.

It was not possible to provide an accurate characterization of the MZI, since it was uncertain whether the measured losses were due to the seismic mass displacement and/or not to the misalignment between the input/output optical fiber and the device. Placing the optical fiber in V-groove made of silicon solved this problem [8]. An unavoidable coupling loss of 2 dB obtained from the coupling light between the optical fiber and the waveguides.

Light of wavelength 1.3 μm was passed through the waveguides fabricated in MZI to check the quality of the waveguides. Figure 4 gives the diffraction image captured using an infrared video camera. So, it is obvious that the quality of the waveguides is excellent.

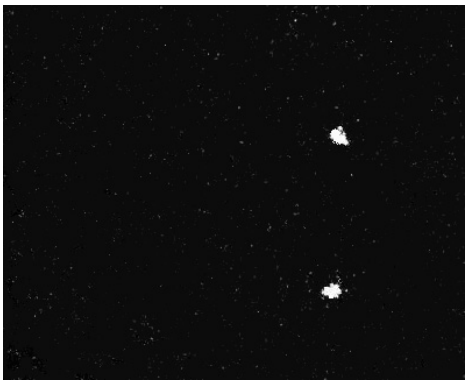

Fig. 4. Diffraction image of output light with wavelength 1.3 μm.

In a further experiment, we tested the performance of the MZI for seismic acceleration detection. The frequency response of the accelerometer was determined using an electrodynamic shaker (GS1020 vibration tester). The accelerometer was bonded to a standard piezoelectric accelerometer; the combination was mounted on top of the shaker with the sensitivity axes of the accelerometers aligned with the direction of motion. The shaker was driven with sinusoidal inputs having frequencies ranging from zero to 8 kHz. The outputs from the accelerometers were recorded using a dual-trace oscilloscope. The transfer function for the accelerometer was calculated from these data. It is plotted in Fig. 5.

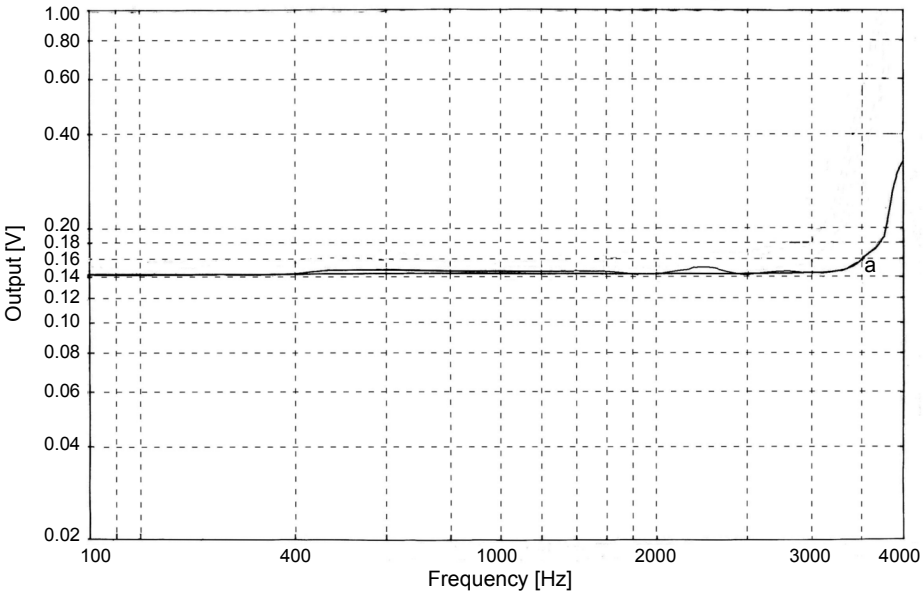

Fig. 5. Frequency response curve of the accelerometer.

In Figure 5, the measured frequency spectra are shown for $a = 0.2g$. The frequency spectrum curve for $a = 0.2g$ is flat in the range of about 100–3000 Hz, which is the useful frequency band for seismic exploration.

5. Conclusions

A hybrid-integrated chip for optical fiber seismic accelerometer with low propagation loss has been designed in this paper. The Mach–Zehnder interferometer (MZI) is designed by analyzing its elements, such as MMI coupler, phase modulator and polarizer, *etc*. The frequency response characteristics of the accelerometer have been measured. It can be seen that the accelerometer has good linear frequency responding characteristic when the frequency is below 3000 Hz, which is in accordance with the operating frequency in high-accuracy seismic exploration.

Acknowledgements – This work was supported by the National Natural Science Foundation of China (No. 40774067) and China Postdoctoral Science Foundation (No. 20100471658).

References

[1] JAKSIC Z., RADULOVIC K., TANASKOVIC D., *MEMS accelerometer with all-optical readout based on twin-defect photonic crystal waveguide*, 24th International Conference on Microelectronics, May 16–19, 2004, Vol. 1, pp. 231–234.

[2] MÜLLER J., *MEMS on silicon for integrated optic metrology and communication systems*, Microsystem Technologies **9**(5), 2003, pp. 308–315.

[3] KALENIK J., PAJĄK R., *A cantilever optical-fiber accelerometer*, Sensors and Actuators A **68**(1–3), 1998, pp. 350–355.

[4] JIA NIAN CAO, YA BIN ZHANG, WEI XIN WANG, TAO HAI, *Research and design of a large-phase shift-fringe-count interferometric fiber-optic accelerometer*, Proceedings of SPIE **5634**, 2004, pp. 315–322.

[5] KE TAO, ZHU TAO, RAO YUNJIANG, XU MIN, SHI CUIHUA, *Accelerometer based on all-fiber Fabry–Perot interferometer formed by hollow-core photonic crystal fiber*, Chinese Journal of Lasers **37**(1), 2010, pp. 171–175.

[6] ZENG N., SHI C.Z., ZHANG M., WANG L.W., LIAO Y.B., LAI S.R., *A 3-component fiber-optic accelerometer for well logging*, Optics Communications **234**(1–6), 2004, pp. 153–162.

[7] GORECKI C., *Preparation of oxinitride optical waveguides with piezoelectric modulation fabricated by silicon micromachining*, Proceedings of SPIE **3825**, 1999, pp. 47–52.

[8] LLOBERA A., PLAZA J.A., SALINAS I., BERGANZO J., GARCIA J., ESTEVE J., DOMINGUEZ C., *Technological aspects on the fabrication of silicon-based optical accelerometer with ARROW structures*, Sensors and Actuators A **110**(1–3), 2004, pp. 395–400.

[9] TANG DONG-LIN, CHEN CAI-HE, CUI YU-MING, DING GUI-LAN, WANG JIN-HAI, XIE JIAN-ZHI, *Spring system of three-component photoelastic fiber optic accelerometer*, Journal of Tianjin University **38**(1), 2005, pp. 61–64.

[10] HU H., RICKEN R., SOHLER W., *Low-loss ridge waveguides on lithium niobate fabricated by local diffusion doping with titanium*, Applied Physics B **98**(4), 2010, pp. 677–679.

[11] HE JUN, XIAO HAO, FENG LEI, LI FANG, ZHANG SONGWEI, LIU YULIANG, *Analysis of phase characteristics of fiber michelson interferometer based on a 3×3 coupler*, Acta Optica Sinica **28**(10), 2008, pp. 1867–1873.

[12] MARCUSE D., *Optimal electrode design for integrated optics modulators*, IEEE Journal of Quantum Electronics **18**(3), 1982, pp. 393–398.

Received March 3, 2011
in revised form July 26, 2011